Electronic Supplementary Information (ESI) for

Heptanickel(II) Double-Cubane Core in Wells-Dawson Heteropolytungstate, $[Ni_7(OH)_6(H_2O)_6(P_2W_{15}O_{56})_2]^{16-}$

Bassem S. Bassil,[a,b,x] Yixian Xiang,[a,x] Ali Haider,[a] Jaime Hurtado,[a] Ghenadie Novitchi,[c] Annie K. Powell,[d,e] A. Martin Bossoh,[f,g] Israël M. Mbomekallé,[f] Pedro de Oliveira,[f] and Ulrich Kortz*[,a]

[a] *Department of Life Sciences and Chemistry, Jacobs University, P.O. Box 750 561, 28725 Bremen, Germany. Fax: +49 421 200 3229; Tel: +49 421 200 3235; E-mail: u.kortz@jacobs-university.de*

[b] *Department of Chemistry, Faculty of Sciences, University of Balamand, P.O. Box 100, Tripoli, Lebanon*

[c] *Laboratoire National des Champs Magnétiques Intenses, CNRS, 38042 Grenoble Cedex 9, France*

[d] *Institute of Inorganic Chemistry, Karlsruhe Institute of Technology (KIT), Engesserstrasse 15, 76131 Karlsruhe, Germany*

[e] *Institute of Nanotechnology, Karlsruhe Institute of Technology (KIT), Hermann-von-Helmholtz Platz 1, 76344 Eggenstein-Leopoldshafen, Germany*

[f] *Laboratoire de Chimie-Physique, Université Paris-Sud, UMR 8000 CNRS, Orsay, F-91405, France*

[g] *Université Félix Houphouët-Boigny, 01 BP V34 Abidjan 01, Côte d'Ivoire*

[x] *These authors contributed equally.*

1. Materials and physical measurements

All reagents were used as purchased without further purification. The trilacunary 15-tungsto-2-phosphate precursor salt $Na_{12}[P_2W_{15}O_{56}]\cdot 24H_2O$ was prepared following a published procedure,[1] and the purity was confirmed by infrared (IR) spectroscopy.

The IR spectra were recorded on a Nicolet Avatar 370 FT-IR spectrophotometer using KBr pellets. The following abbreviations were used to assign the peak intensities: w = weak, m = medium, and s = strong. Elemental analysis was performed by Service Central d'Analyse, Solaize, France. Thermogravimetric analysis (TGA) was carried out on a TA Instruments SDT Q600 thermobalance with a 100 mL min^{-1} flow of nitrogen; the temperature was ramped from 25 to 600 °C at a rate of 5 °C min^{-1}.

2. X-ray crystallography

A single crystal of **1a** was mounted on a Hampton cryoloop in light oil for data collection at 100 K. Indexing and data collection were performed on a Bruker D8 SMART APEX II CCD diffractometer with kappa geometry and Mo Kα radiation (graphite monochromator, λ = 0.71073 Å). Data integration was performed using SAINT.[2] Routine Lorentz and polarization corrections were applied. Multiscan absorption corrections were performed using SADABS.[3] Direct methods (SHELXS97) successfully located the tungsten atoms, and successive Fourier syntheses (SHELXL14) revealed the remaining atoms.[4] Refinements were full matrix least-squares against $|F^2|$ using all data. In the final refinement, all non-disordered heavy atoms (W, Ni, P, Cs, Na) were refined anisotropically; oxygen atoms and disordered counter cations were refined isotropically. No hydrogen atoms were included in the models.

For overall consistency we show in the CIF file the same formula unit as in the main text, with the exact numbers of counter cations and crystal waters (based on elemental analysis and TGA), as this reflects the true bulk composition of **1a**. Crystallographic data are summarized in Table S1.

Table S1. Crystal data and structural refinement for **1a**.

Compound	**1a**
Formula	$Na_{14.5}Cs_{1.5}[Ni_7(OH)_6(H_2O)_6(P_2W_{15}O_{56})_2]\cdot 56H_2O$
Formula weight, g/mol	9594.10
Crystal system	Triclinic
Space group (Number)	*P-1* (2)
a, Å	12.7488(4)
b, Å	12.7765(4)
c, Å	25.7791(10)
α, °	92.399(2)
β, °	101.831(2)
γ, °	104.172(2)
Volume, $Å^3$	3966.0(2)
Z	1
D_{calc}, g/cm^3	4.017
Absorption coefficient	23.014
F(000)	4288
Crystal size, mm	0.143 x 0.126 x 0.012
Theta range for data collection, °	3.41- 28.28
Completeness to Θ_{max}, %	98.7
Index ranges	-16<=h<=16, -16<=k<=17, -34<=l<=34
Total Reflections	212129
Independent Reflections	19379
Calculated Reflections (I>2σ)	15027
R(int)	R(int) = 0.0913
Data / restraints / parameters	15027 / 0 / 587
Goodness-of-fit on F2	1.002
R_1 [a]	0.0676
wR_2 [b]	0.1678
e Density max / min, e. $Å^{-3}$	4.762 / -3.842

[a] $R_1 = \sum | |F_o| - |F_c| | / \sum |F_o|$. [b] $wR_2 = [\sum w (F_o^2 - F_c^2)^2 / \sum w(F_o^2)^2]^{1/2}$

3. Bond valence sum calculations

Bond valence sum (BVS) calculations for the oxygen atoms in polyanion **1** were performed on a program copyrighted by Chris Hormillosa & Sean Healy and distributed by I. D. Brown.[5] Table S2 presents the BVS values for the protonated oxygens in **1**. The total charge of **1** is therefore 22-, which is balanced by sodium and cesium counter cations in the solid state.

Table S2. BVS values for the protonated oxygens in **1**.

Bridging oxygens (μ_3-O-NiNiNi)	**BVS value**	**Terminal oxygens (Ni-O)**	**BVS value**
O37N[#]	1.07	O2[*]	0.30
O27N[#]	1.09	O6[*]	0.33
O37I[#]	1.12	O4[*]	0.33

[#] monoprotonated oxygen (OH^-)
[*] diprotonated oxygen (H_2O)

4. Polyhedral representation and Ni_7 core structure

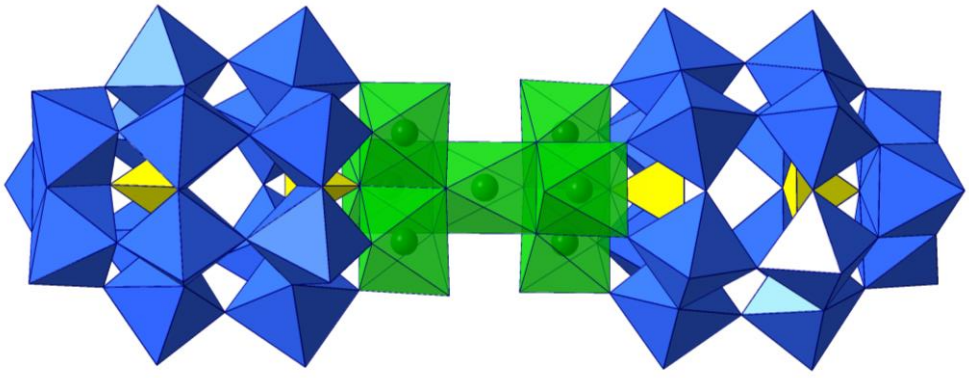

Figure S1. Polyhedral representation of **1**. Color code for polyhedra: NiO_6 green, WO_6 blue, PO_4 yellow.

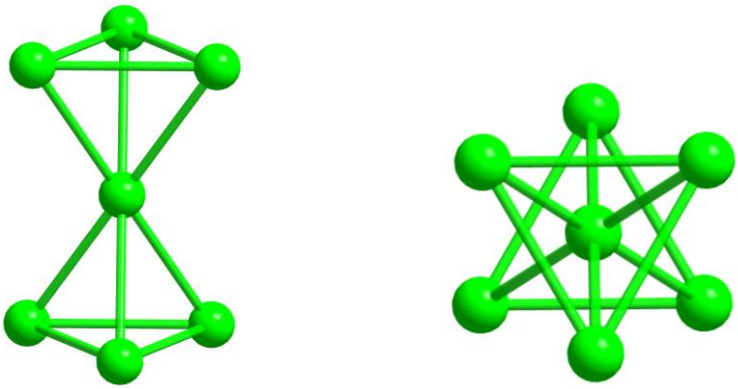

(a) **(b)**

Figure S2. Structure of the double-cubane Ni_7 core from side (a) and top (b) view.

5. IR spectroscopy

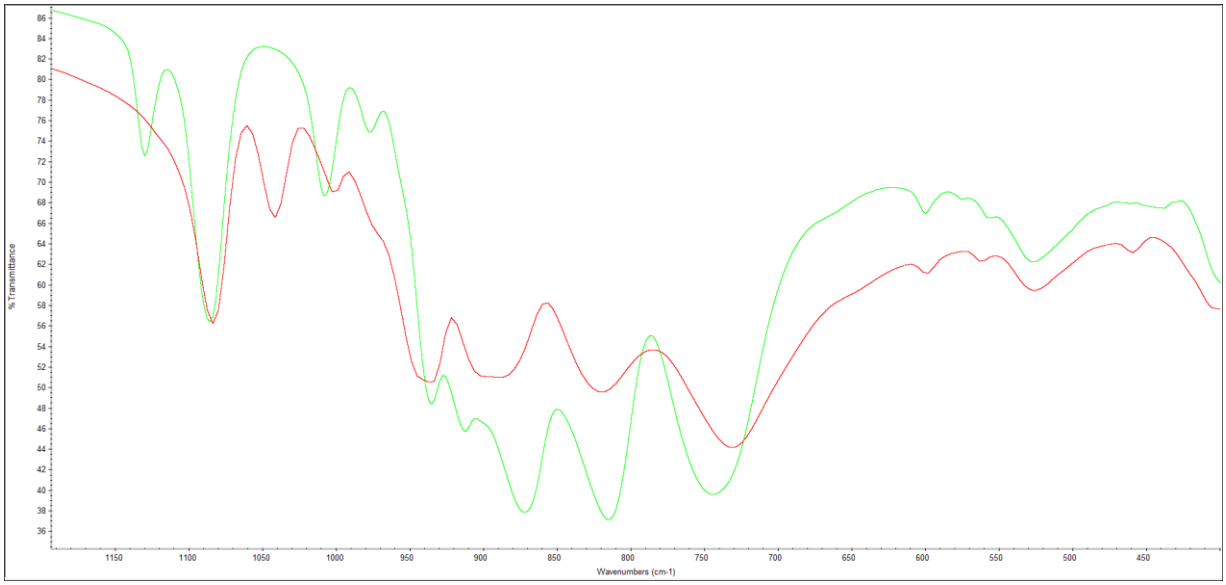

Figure S3. FT-IR spectrum of **1a** (red) compared to $Na_{12}[P_2W_{15}O_{56}]\cdot 24H_2O$ (green)**.**

6. Thermogravimetric analysis

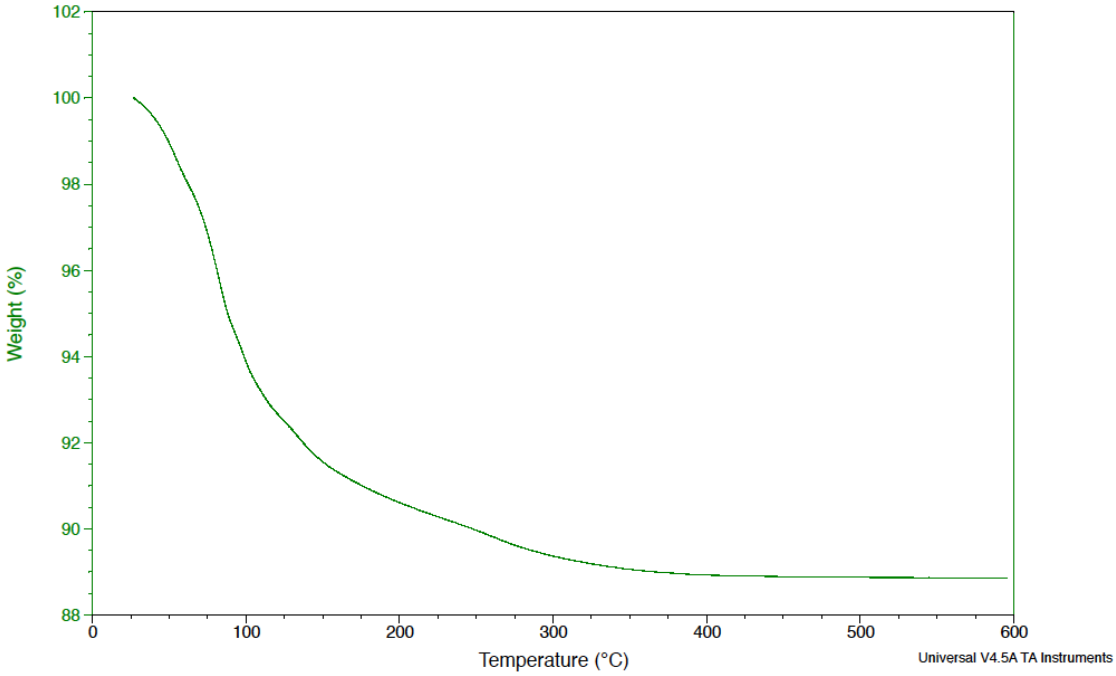

Figure S4. Thermogram of **1a** from room temperature to 600 °C.

7. NMR spectroscopy

The ^{31}P NMR spectrum of **1a** dissolved in H_2O/D_2O was recorded in a 5 mm tube on a 400 MHz (JEOL, Model ECS) instrument at room temperature with a resonance frequency of 161.834 MHz, and the chemical shift is reported with respect to 85% H_3PO_4.

8. Magnetism

Magnetic susceptibility data (1.8-300 K) were collected on powdered samples of **1a** using a SQUID magnetometer (Quantum Design MPMS-XL), applying a magnetic field of 0.1 T. All data were corrected for the contribution of the sample holder and the diamagnetism of the samples, estimated from Pascal's constants.[6] Magnetic data analysis was carried out by calculations of energy levels associated with the spin Hamiltonians presented in the text, and with the MAGPACK program package.[7]

Table S3. Ni-O-Ni bond angles within the heptanickel-oxo double-cubane cluster in **1**.

	a	*b*	*c*	Angle *abc*	average angle
Ni1-Ni7	Ni1	O37N	Ni7	96.323	**96.830**
	Ni1	O27N	Ni7	97.336	
Ni2-Ni7	Ni2	O27N	Ni7	96.669	**96.717**
	Ni2	O37I	Ni7	96.765	
Ni3-Ni7	Ni3	O37I	Ni7	97.625	**97.780**
	Ni3	O37N	Ni7	97.935	
Ni1-Ni2	Ni2	O20	Ni1	92.542	**97.122**
	Ni1	O27N	Ni2	101.702	
Ni1-N3	Ni3	O22	Ni1	93.109	**97.438**
	Ni1	O37N	Ni3	101.767	
Ni2-Ni3	Ni3	O20	Ni2	93.048	**97.209**
	Ni2	O37I	Ni3	101.369	

Table S4. Best simulation parameters for models **A** - **C** according to Hamiltonian (1).

	A ($J_1 = J_2$)	**B** ($J_1 < J_2$)	**C** ($J_1 > J_2$)
J_1 (cm^{-1})	5.5	4.2	6.4
J_2 (cm^{-1})	5.5	7.5	3.5
G	2.29	2.29	2.29
R	2×10^{-3}	6×10^{-4}	9×10^{-4}

$$H=-2J_1(S_1S_7+ S_2S_7 + S_3S_7 + S_4S_7 + S_5S_7 + S_6S_7)- -2J_2(S_1S_2 +S_2S_3 + S_1S_3 + S_4S_5 + S_5S_6 + S_4S_6) \quad (1),$$

where $S_i = 1$.

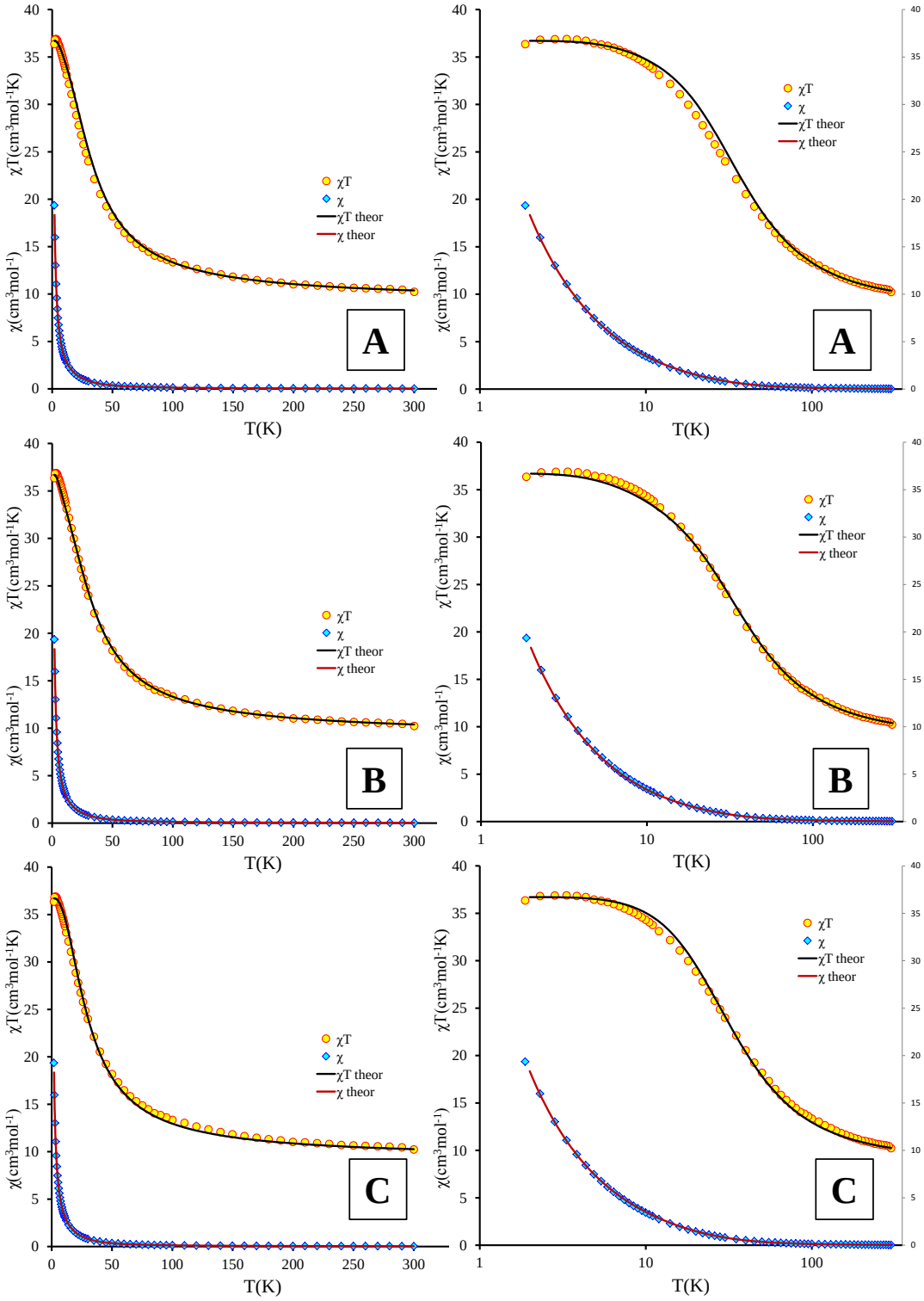

Figure S5. χT and χ versus T plots for **1a**. The solid lines correspond to the simulation for models **A** - **C** according to Hamiltonian (1) with parameters presented in Table S4.

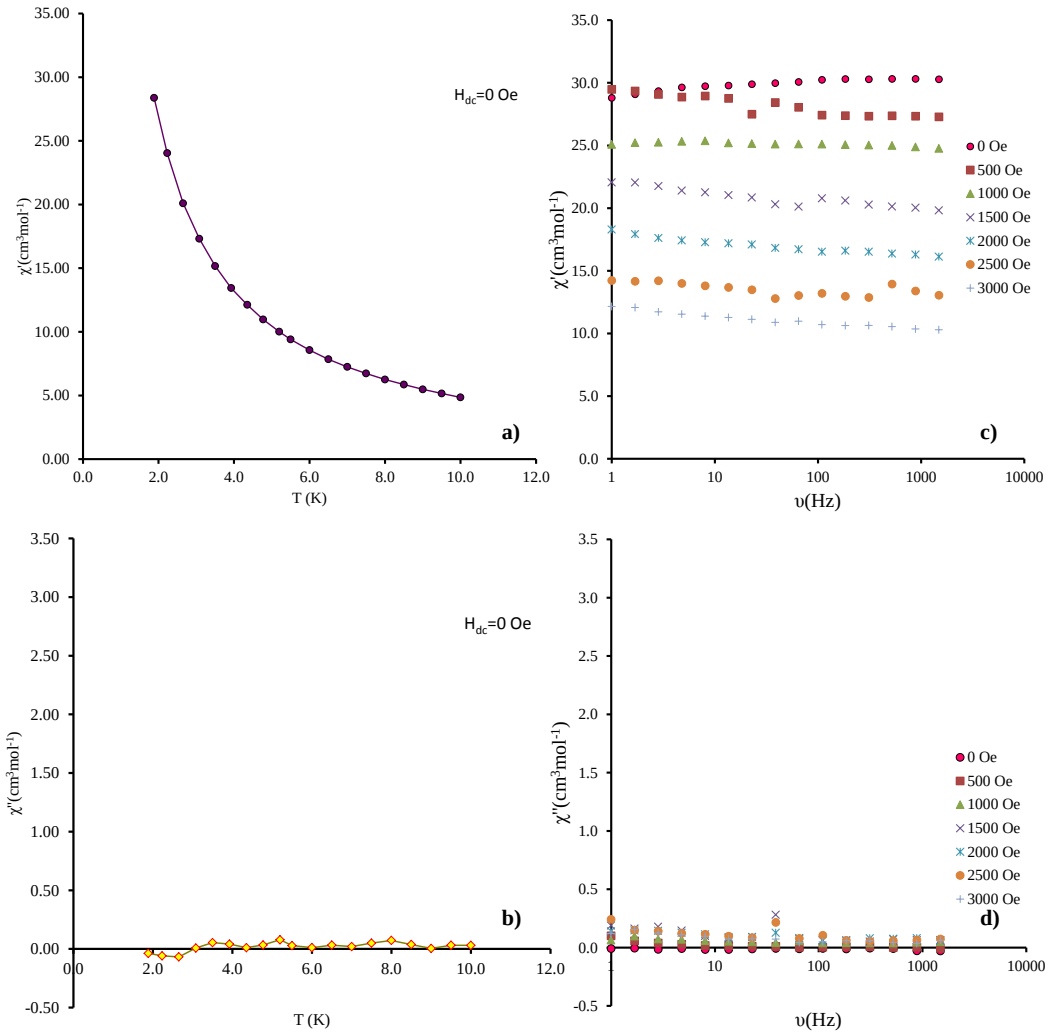

Figure S6 Variable temperature (a, b) and variable frequency (c, d at T = 1.8 K) AC susceptibility data for **1a** at indicated DC fields.

9. Electrochemistry

Electrochemical data were obtained using an EG & G 273 A potentiostat driven by a PC with the M270 software. A one-compartment cell with a standard three-electrode configuration was used for cyclic voltammetry (CV) experiments. The reference electrode was a saturated calomel electrode (SCE) and the counter electrode a platinum gauze of large surface area; both electrodes were separated from the bulk electrolyte solution via fritted compartments filled with the same electrolyte. The working electrode was a 3 mm OD glassy carbon disc or a *ca.* $10 \times 10 \times 2$ mm^3 stick (GC, Le Carbone-Lorraine, France). The pre-treatment of this electrode before each experiment has been described elsewhere.[8] The concentration of **1** was 5.0×10^{-4} M. Prior to each experiment, solutions were thoroughly de-aerated for at least 30 min with pure Ar. A positive pressure of this gas was maintained during subsequent work. All CVs were recorded at a scan rate of 10 mV s^{-1} and potentials are quoted against the saturated calomel electrode (SCE) unless otherwise stated. All experiments were performed at room temperature, which was controlled and fixed for the laboratory at 20 °C. Results were very reproducible from one experiment to another and slight variations observed for successive runs are rather attributed to the uncertainty associated with the detection limit of our equipment (potentiostat, hardware and software), and not to the working electrode pre-treatment nor to possible fluctuations in temperature.

The composition of the various media was as follows: for pH 3.0, 0.2 M Na_2SO_4 + H_2SO_4; for pH 5.0, 0.4 M $NaCH_3COO$ + CH_3COOH. They were prepared with pure water obtained with a Milli-Q Intregral 5 purification set. All reagents were of high-purity grade and were used as purchased without further purification: H_2SO_4 (Sigma Aldrich), anhydrous Na_2SO_4 (Riedel-de Haën), $NaCH_3COO.3H_2O$ (Sigma Aldrich), and CH_3COOH (Carlo Erba). The stability of **1** in these media was studied by monitoring the evolution of the UV-visible spectra and the CVs. The UV-visible spectra were recorded on a Perkin-Elmer Lambda 19 spectrophotometer with 5×10^{-5} M solutions of **1**. Matched 10.00 mm optical path quartz cuvettes were used.

The CVs of **1** and $[P_2W_{15}O_{56}]^{12-}$ in 0.2 M Na_2SO_4 + H_2SO_4 (pH 3.0) were compared, despite the fact that $[P_2W_{15}O_{56}]^{12-}$ is rather unstable in this medium. Therefore, the CV of $[P_2W_{15}O_{56}]^{12-}$ was obtained immediately after dissolution of the compound, so that

its relatively rapid decay at pH 3 [9] was kept to a minimum (Figure S7A). The same experiment with compound **1** reveals a much better stability with time (Figure 7B). The CV for **1** beyond pH 3 showed poorly defined waves, and the polyanion decomposed after a few hours. These results are complementary and confirm those obtained by UV-visible spectrophotometry, which allowed us to follow the evolution of the UV-visible spectra of the different compounds in solution as a function of time, and to assess their stability in the media used in this study.

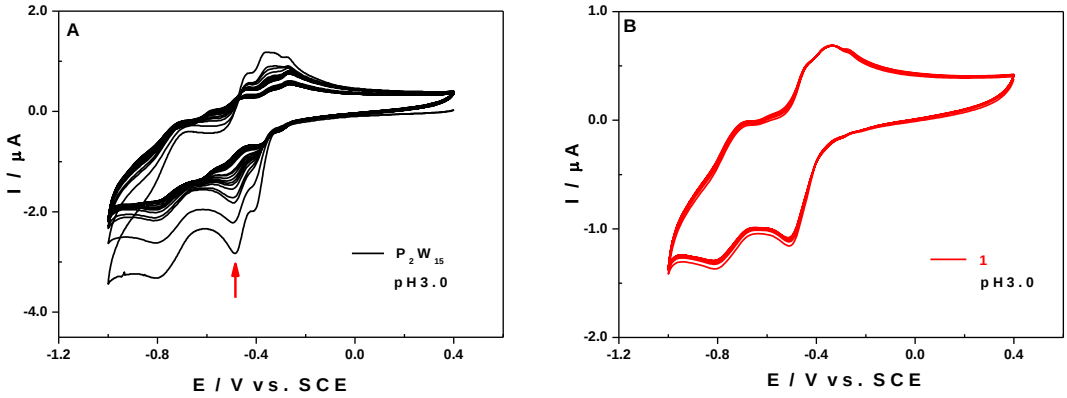

Figure S7. Consecutive CVs (5 min between two cycles) of $[P_2W_{15}O_{56}]^{12-}$ (A) and **1** (B) in 0.2 M Na_2SO_4 + H_2SO_4 / pH 3.0. POM concentration: 10^{-4} M. Working electrode: glassy carbon; reference electrode: SCE. Scan rate: 10 mV s^{-1}. The CVs of **1** remain superimposable after 5 hours of cycling.

Table S5. Reduction peak potentials, E_{pc}, in V vs. SCE, for **1** and $[P_2W_{15}O_{56}]^{12-}$ as taken from the cyclic voltammograms obtained at a scan rate of 10 mV s^{-1} with a glassy carbon working electrode at pH 3.

pH 3	E_{pc1}	E_{pc2}	E_{pc3}
$[P_2W_{15}O_{56}]^{12-}$	-0.410	-0.490	-0.790
1	-0.430[a]	-0.490	-0.790

[a] shoulder on the main wave

Table S6. Catalytic efficiency, CAT, and current densities, J, at -0.97 V vs. SCE, of **1** *versus* $[(NiOH_2)_2Ni_2(P_2W_{15}O_{56})_2]^{16-}$ (**$Ni_4P_4W_{30}$**) in 0.2 M Na_2SO_4 + H_2SO_4 (pH 3.0) with respect to the reduction of nitrate ions on a glassy carbon electrode. The cyclic voltammograms were obtained at a scan rate of 2 mV s^{-1}. CAT = 100 × {[I(POM + NO_3^-) – I(POM)]/ I(POM)}.[10]

(at -0.97 V vs. SCE)	**1**	**$Ni_4P_4W_{30}$**
CAT (%)	188	113
J ($\mu A.cm^{-1}$)	-69.7	-51.4

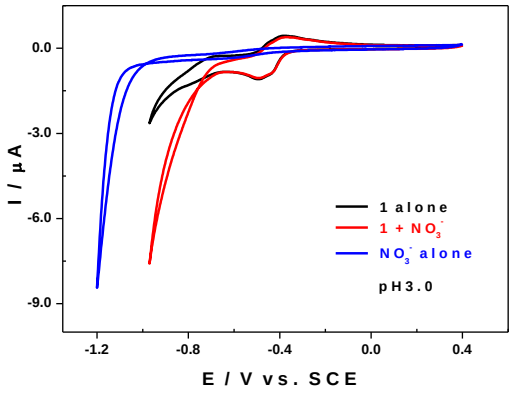

Figure S8. CVs of **1** in the absence (black) and presence (red) of nitrate ions in 0.2 M Na_2SO_4 + H_2SO_4 (pH 3.0), compared with the electro-reduction of the same amount of nitrate ions alone. POM concentration: 10^{-4} M; nitrate ions concentration: 5.10^{-2} M. Working electrode: glassy carbon; reference electrode: SCE. Scan rate: 2 mV s^{-1}.

10. References

[1] R. G. Finke, M. W. Droege, P. J. Domaille, *Inorg. Chem.,* 1987, **26**, 3886.

[2] SAINT; Bruker AXS Inc.: Madison, WI, 2007.

[3] (a) G. M. Sheldrick, *Acta Crystallogr.,* 2007, **A64**, 112. (b) G. M. Sheldrick, SADABS; University of Göttingen: Göttingen, Germany, 1996.

[4] G. M. Sheldrick, SHELX, Program for Solution of Crystal Structures; University of Göttingen: Göttingen, Germany, 2015.

[5] I. D. Brown, D. Altermatt, *Acta Crystallogr.*, 1985, **B41**, 244.

[6] a) P. Pascal, *Ann. Chim. Phys.,* 1910, **19**, 5; b) Molecular Magnetism, O. Kahn, VCH Publishers, Inc., New York, Weinheim, Cambridge, 1993.

[7] J. J. Borras-Almenar, J. M. Clemente-Juan, E. Coronado, B. S. Tsukerblat, *J. Comp. Chem.,* 2001, **22**, 985.

[8] N. Vila, P. A. Aparicio, F. Sécheresse, J. M. Poblet, X. López, I. M. Mbomekalle, *Inorg. Chem.* 2012, **51**, 6129.

[9] R. Contant, G. Hervé, *Rev. Inorg. Chem.* 2002, **22**, 63.

[10] C. P. Andrieux, J. M. Dumas-Bouchiat, J. M. Savéant, *J. Electroanal. Chem.* 1980, **113**, 1.